Supercond. Sci. Technol. 3 (1990) 128–133. Printed in the UK

The optimum percentage of Pb and the appropriate thermal procedure for the preparation of the 110 K $Bi_{2-x}Pb_xSr_2Ca_2Cu_3O_y$ superconductor

M Pissas, D Niarchos, C Christides and M Anagnostou
National Center for Scientific Research 'Demokritos', Institute of Materials Science, 153 10 Aghia Paraskevi Attikis, Greece

Received 4 October 1989, in final form 18 December 1989

Abstract. The high-T_c phase (110 K) of the $Bi_{2-x}Pb_xSr_2Ca_2Cu_3O_y$ system has been synthesised and the role of Bi/Pb substitution has been studied extensively using x-ray diffraction studies, electrical resistivity and magnetisation measurements and scanning electron microscopy. It was found that the best results were obtained for $x = 0.2$–0.3 and that a 'step sintering process' is necessary for a better control of the thermal process.

1. Introduction

Following the discovery by Bednorz and Müller [1] of a high transition temperature (T_c) in the system $La_{2-x}Sr_xCuO_4$ with $x = 0.15$ and the achievement of a $T_c = 90$ K by Wu *et al* [2] in the system $REBa_2Cu_3O_{6+x}$, where RE represents rare earth or Y, Michel *et al* [3] reported a T_c of 10 K for the system Bi–Sr–Cu–O. The addition of Ca in the Bi–Sr–Cu–O system led Maeda *et al* [4] to the discovery of bulk superconductivity at 85 K and evidence of superconductivity at 110 K. We now know that there are three superconducting phases having the general formula $Bi_2Sr_2Ca_{n-1}Cu_nO_y$ where $n = 1, 2, 3$ and that these phases have transition temperatures of 10, 80, 110 K respectively.

A common characteristic of these Bi-based superconductors is the presence of two Bi–O layers which are 3.2 Å apart and are shifted with respect to each other (crystallographic shear) along the diagonal direction of the perovskite subcell.

The structure of the 10 K (2202) phase is orthorhombic with one layer of CuO_2 per formula unit and $a = 5.362$ Å, $b = 5.374$ Å, $c = 24.622$ Å [5]. This phase additionally possesses an incommensurate superstructure along the $a + b$ direction.

The structure of the 80 K (2212) phase is orthorhombic with $a = 5.413$ Å and $c = 30.871$ Å [6]. The structure contains one layer of Ca sandwiched between two CuO_2, two Sr–O and two Bi–O layers. The phase also has a superstructure along the b direction.

The $n = 3$ member (2223) of the series is equivalent to the (2212) member with the addition of one layer of Cu–O and one Ca layer in the perovskite block of the structure. One characteristic of the (2223) phase is the presence of stacking faults [7]. It also possesses superstructure along the b direction.

By substitution of Bi with Tl, and Sr with Ba, a new series of phases is formed with the general formula $Tl_2Ba_2Ca_{n-1}Cu_nO_y$ where $n = 1, 2, 3$ and $T_c = 80, 100, 120$ K, respectively [8]. Unlike the phases with thallium, which can be easily prepared for every n, the preparation of phase $Bi_2Sr_2Ca_2Cu_3O_y$ with $T_c = 110$ K has some difficulties. Partial substitution of Bi by Pb aids the formation of the 110 K phase [9–14]. In order to make samples having a large percentage of 110 K phase with respect to the 80 K phase, we should heat treat the material for a prolonged time close to its melting point (≈ 880 °C). Recently, it was reported [15, 16] that the substitution of Bi with Pb and Sb in the material, with starting stoichiometry $Bi_{1.7}Pb_{0.2}Sb_{0.1}Sr_2Ca_2Cu_{2.8}O_y$, is capable of giving the 110 K phase when annealed for three days at 850–865 °C, compared to 10 days annealing time needed to prepare samples of the same quality substituting Bi by Pb only.

In this paper we report in detail about the factors which favour the formation of the 110 K phase. Specifically, we report results obtained for the series $Bi_{2-x}Pb_xSr_2Ca_2Cu_3O_y$ as a function of Pb substitution and thermal treatment, which must be followed to obtain an almost pure phase with $T_c(R = 0) \approx 103$ K. Although many papers have dealt with this problem we believe that our work, through a systematic study of x-rays, magnetisation and resistivity measurements at different x values, will show the mechanism of transformation of one phase (80 K) to the other (110 K).

0953-2048/90/030128 + 06 $03.50 © 1990 IOP Publishing Ltd

2. Experimental procedure

A series of samples with starting composition $Bi_{2-x}Pb_xSr_2Ca_2Cu_3O_y$ ($x = 0.1$, 0.2, 0.25, 0.3, 0.4 and 0.5) were prepared by conventional ceramic processing by thoroughly mixing Bi_2O_3, PbO_2, $SrCO_3$, $CaCO_3$ and CuO of at least 99.9% purity. The mixture of starting materials was pressed into 2 cm diameter disc-shape pellets with thickness 2 mm and calcinated at 770 °C for 49 h. During this stage the samples were reground, mixed and recompacted a number of times in order to obtain good homogeneity. This preheating was necessary to avoid partial melting in the next stages of the thermal process, where the temperature is higher. In the second stage of the thermal process the samples were pressed into 2 cm diameter pellets and underwent sintering with durations and temperatures given in table 1. All stages of the thermal process took place in air (open furnace). The initial stoichiometry, the thermal process and the cooling process for all the samples are given in table 1.

The x-ray diffraction measurements were made on a Philips x-ray powder diffractometer using Co Kα radiation. The magnetic properties of the samples were studied in the range 4.2 to 300 K and in applied fields of 50–100 G using a PAR155 vibrating sample magnetometer. The samples used for the magnetic measurements were in powder form.

Electrical resistance measurements as a function of temperature were taken by a computerised system, in a standard four-probe configuration using silver ink to make the electrical contacts on the sample.

The microstructural characterisation was performed using scanning electron microscopy (SEM) with a Philips 515. The compositional analysis of the samples was performed with an energy dispersive x-ray EDAX 9900 system with a Si(Li) counter of 155 eV (Mn Kα) energy resolution and a Be window with a width of 7.5 μm. The energy of the beam was 30 keV.

3. Results and discussion

3.1. X-ray diffraction spectra

In all the steps of the thermal procedure, except the last one, the sample with $x = 0.1$ ($Bi_{1.9}Pb_{0.1}Sr_2Ca_2Cu_3O_y$) did not show traces of the (2223) phase in the x-ray diffraction pattern unless [7] the temperature was raised to 880–885 °C.

For the sample with $x = 0.2$ ($Bi_{1.8}Pb_{0.2}Sr_2Ca_2Cu_3O_y$) we can see the transformation of the (2212) phase into the 2223 phase (figure 1). In conjunction with table 1 we can conclude that in order to start the transformation of the 2212 into the 2223 phase, it is necessary to heat the sample at 860 °C for at least 3–4 days (figure 1(*a*)). A subsequent increase of the temperature to 870 °C and annealing for 7 days leads to a sample with the 2223 and 2212 phases. The sample at this stage, as in the previous one, presents strong preferred orientation, thus making the extraction of conclusions related to the percentage of each phase difficult. Further increase of the temperature to 875 °C leads, after 8 days, to an improved 2223/2212 ratio and to an increase of the width of the peaks in the x-ray spectrum (figure 1(*c*)).

In figures 2(*a*), (*b*) and (*c*) the transformation of the 2212 to the 2223 phase for the sample with $x = 0.25$ ($Bi_{1.75}Pb_{0.25}Sr_2Ca_2Cu_3O_y$) is shown. It can be seen that a significant amount of the 2212 phase has been transformed into the 2223 phase in figure 2(*a*). Further

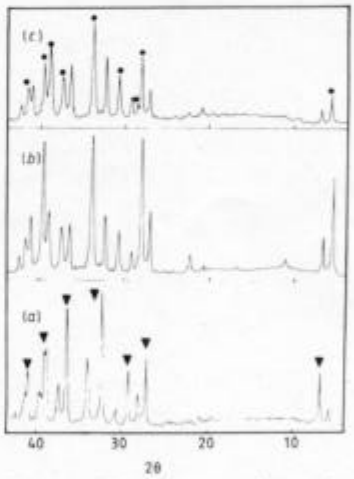

Figure 1. The x-ray diffraction patterns for sample $Bi_{1.8}Pb_{0.2}Sr_2Ca_2Cu_3O_y$ at different steps of the thermal process. (*a*) At the end of step 4; (*b*) at the end of step 5, (*c*) at the end of step 6. The symbol ● identifies the peaks of 2223 phase and the symbol ▼ identifies the peaks of 2212 phase.

Table 1. Nominal stoichiometry and the thermal process for all the compounds.

Nominal initial composition					Step 1		Step 2		Step 3		Step 4		Step 5		Step 6	
Bi	Pb	Sr	Ca	Cu	Time (h)	T (°C)	Time (h)	T (°C)	Time (h)	T (°C)	Time (h)	T (°C)	Time (h)	T (°C)	Time (h)	T (°C)
1.9	0.1	2	2	3	49	770	46	845	46	855	74	860	183	870	192	875
1.8	0.2	2	2	3	49	770	46	845	46	855	74	860	183	870	192	875
1.75	0.25	2	2	3	44	765	40	795	72	855	74	865	192	870	168	875
1.7	0.3	2	2	3	49	770	46	845	46	855	74	860	183	870	192	875
1.6	0.4	2	2	3	49	770	46	845	46	855	74	860	183	870	192	875
1.5	0.5	2	2	3	49	770	46	845	46	855	74	860	183	870	192	875

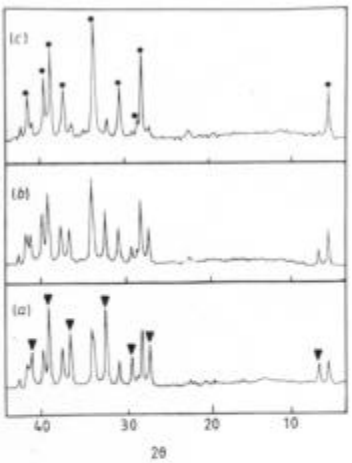

Figure 2. The x-ray diffraction patterns for sample $Bi_{1.75}Pb_{0.25}Sr_2Ca_2Cu_3O_y$ at different steps of the thermal process. (*a*) At the end of step 4, (*b*) at the end of step 5, (*c*) at the end of step 6. The symbol ● identifies the peaks of 2223 phase and the symbol ▼ identifies the peaks of 2212 phase.

annealing at 870 °C for 7 days and at 875 °C for 8 days gives a sample containing nearly all 2223 phase.

The x-ray patterns for the different stages of the heat treatment of the sample with $x = 0.3$ ($Bi_{1.7}Pb_{0.3}Sr_2Ca_2Cu_3O_y$) are shown in figures 3(*a*), (*b*) and (*c*). For the previous two samples at the final stage we have a sample with a large amount of the 2223 phase.

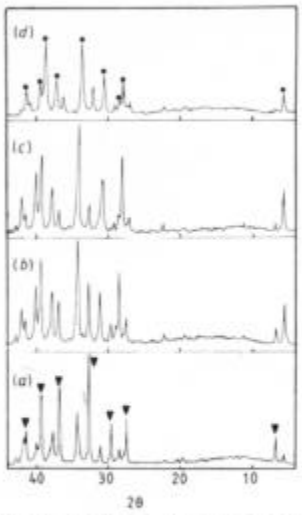

Figure 3. The x-ray diffraction patterns for sample $Bi_{1.7}Pb_{0.3}Sr_2Ca_2Cu_3O_y$ at different steps of the thermal process. (*a*) At the end of step 4, (*b*) at the end of step 5, (*c*) at the end of step 6, (*d*) 100 h after the beginning of step 6. The symbol ● identifies the peaks of 2223 phase and the symbol ▼ identifies the peaks of 2212 phase.

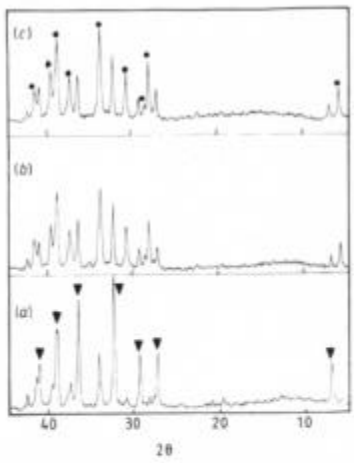

Figure 4. The x-ray diffraction patterns for sample $Bi_{1.6}Pb_{0.4}Sr_2Ca_2Cu_3O_y$ at different steps of the thermal process. (*a*) At the end of step 4, (*b*) at the end of step 5, (*c*) at the end of step 6. The symbol ● identifies the peaks of 2223 phase and the symbol ▼ identifies the peaks of 2212 phase.

In figures 4(*a*), (*b*) and (*c*) the x-ray patterns, at different stages of the heat treatment, for the sample with $x = 0.4$ ($Bi_{1.6}Pb_{0.4}Sr_2Ca_2Cu_3O_y$) are shown. It is apparent for $x \geqslant 0.4$ Pb that the conditions for the preparation of the 2223 phase become very difficult. In figure 4(*a*) the existence of a small amount of phase 2223 together with the main 2212 phase is shown. The final sample also contains a significant amount of the 2212 phase (figure 4(*c*)). As the concentration of Pb increases to $x = 0.5$ ($Bi_{1.5}Pb_{0.5}Sr_2Ca_2Cu_3O_y$) the preparation of the 2223 phase becomes more difficult (figure 5(*b*)). The 2212 phase dominates over the 2223 phase even on stage 5 of the heat treatment and only on stage 6 does the percentage of 2223 phase become comparable to the percentage of the 2212 phase (figure 5(*c*)).

The lattice constants, determined from the x-ray diagrams, are constant within experimental error for all the Pb concentrations considered in this study (table 2).

3.2. Resistivity measurements

Resistivity versus temperature for all samples was measured at a current of 10 mA. The current density

Table 2. Crystallographic lattice parameters for the $Bi_{2-x}Pb_xSr_2Ca_2Cu_3O_y$ series. The indexing corresponds to the I4/mmm space group. The *a* and *c* for $x = 0.0$ were taken from the work of Tarascon *et al* [7].

x	*a* (Å)	*c* (Å)
0.0	3.81	37.10
0.2	3.81	36.95
0.25	3.81	37.07
0.3	3.82	37.17
0.4	3.81	37.20
0.5	3.81	37.14

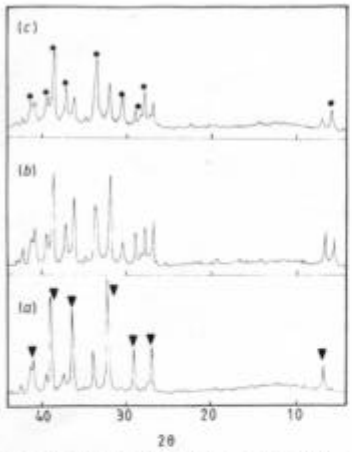

Figure 5. The x-ray diffraction patterns for sample $Bi_{1.5}Pb_{0.5}Sr_2Ca_2Cu_3O_y$ at different steps of the thermal process. (*a*) At the end of step 4, (*b*) at the end of step 5, (*c*) at the end of step 6. The symbol ● identifies the peaks of 2223 phase and the symbol ▼ identifies the peaks of 2212 phase.

was estimated to be about 166 mA cm^{-2} in the sintered sample. Figure 6 shows the resistivity versus temperature plot for the samples with $x = 0.1$, 0.2, 0.25, 0.3, 0.4 and 0.5. All samples have a T_c onset at about 110 K. Zero resistivity for temperatures above 100 K was observed in the samples with $x = 0.2$, 0.3, 0.4. The sample with $x = 0.5$ (figure 6) has a significant fall in resistivity around 105 K and zero resistivity below 77 K.

The sample with $x = 0.25$ in figure 6 has a wide transition with T_c onset at 110 K and zero resistivity around 96 K. This result is very strange because the sample has approximately 90% 2223 phase and yet the transition in resistivity has two steps. Another fact worth mentioning is the small resistivity of the $x = 0.1$ sample above 110 K compared with the other samples. The percentage of the 110 K phase in this sample is very small.

A correlation between the $T_c(R = 0)$ and the percentage of Pb which substitutes Bi cannot be made because the microstructure of the material (size, manner of grain contact etc) should be taken into account.

The resistivity at the normal state for all the samples increases linearly with temperature, indicating a metallic behaviour. In figure 6 we can see the two different resistivity curves for the $Bi_{1.7}Pb_{0.3}Sr_2Ca_2Cu_3O_y$ sample sintered for two different time intervals at 875 °C (100 and 192 h respectively). A remarkable decrease in resistivity with increasing sintering time has been observed.

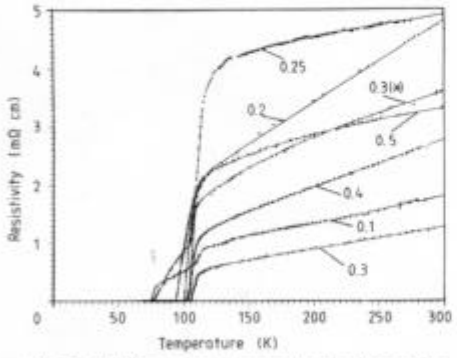

Figure 6. Resistivity against temperature for the series $Bi_{2-x}Pb_xSr_2Ca_2Cu_3O_y$ with $x = 0.1$, 0.2, 0.25, 0.3, 0.4 and 0.5. The curve with 0.3 (*) shows the resistivity of the sample with $x = 0.3$, 92 h before the end of step 6. The rest of the measurements were taken at the end of the thermal process.

3.3. Magnetic measurements

The magnetic measurements on all samples were taken in the field cooling mode (Meissner effect) and the samples used were in powder form. In figure 7 the DC susceptibility curves for all the $Bi_{2-x}Pb_xSr_2Ca_2Cu_3O_y$ samples with $x = 0.1$, 0.2, 0.25, 0.3, 0.4, 0.5 are presented. The T_c onsets are around 110 K, in agreement with the resistivity measurements. The sample with $x = 0.1$ is dominated by the 2212 phase and consequently the major diamagnetic contribution comes from a 77 K transition. The magnitude of the change in the diamagnetic signal in this temperature range can be associated qualitatively to the percentage of the 2212 phase. Specifically we can find the percentage of Pb for which we have the smaller change in the diamagnetic signal, and consequently the smaller amount of the 2212 phase. From figure 7 we can see that the smaller change of the diamagnetic signal is for $x = 0.25$ and 0.30. The above results agree with results from the x-ray patterns.

3.4. Scanning electron microscopy studies

The morphologies of the superconducting compounds are shown in the scanning electron micrographs in figure 8. The micrographs shown correspond to com-

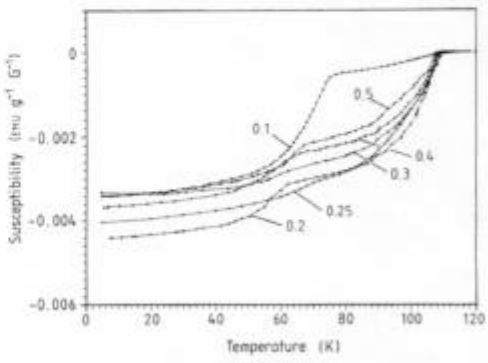

Figure 7. DC susceptibility against temperature in a field-cooling mode for the series $Bi_{2-x}Pb_xSr_2Ca_2Cu_3O_y$ with $x = 0.1$, 0.2, 0.25, 0.3, 0.4 and 0.5. All the measurements were taken at the end of the thermal process.

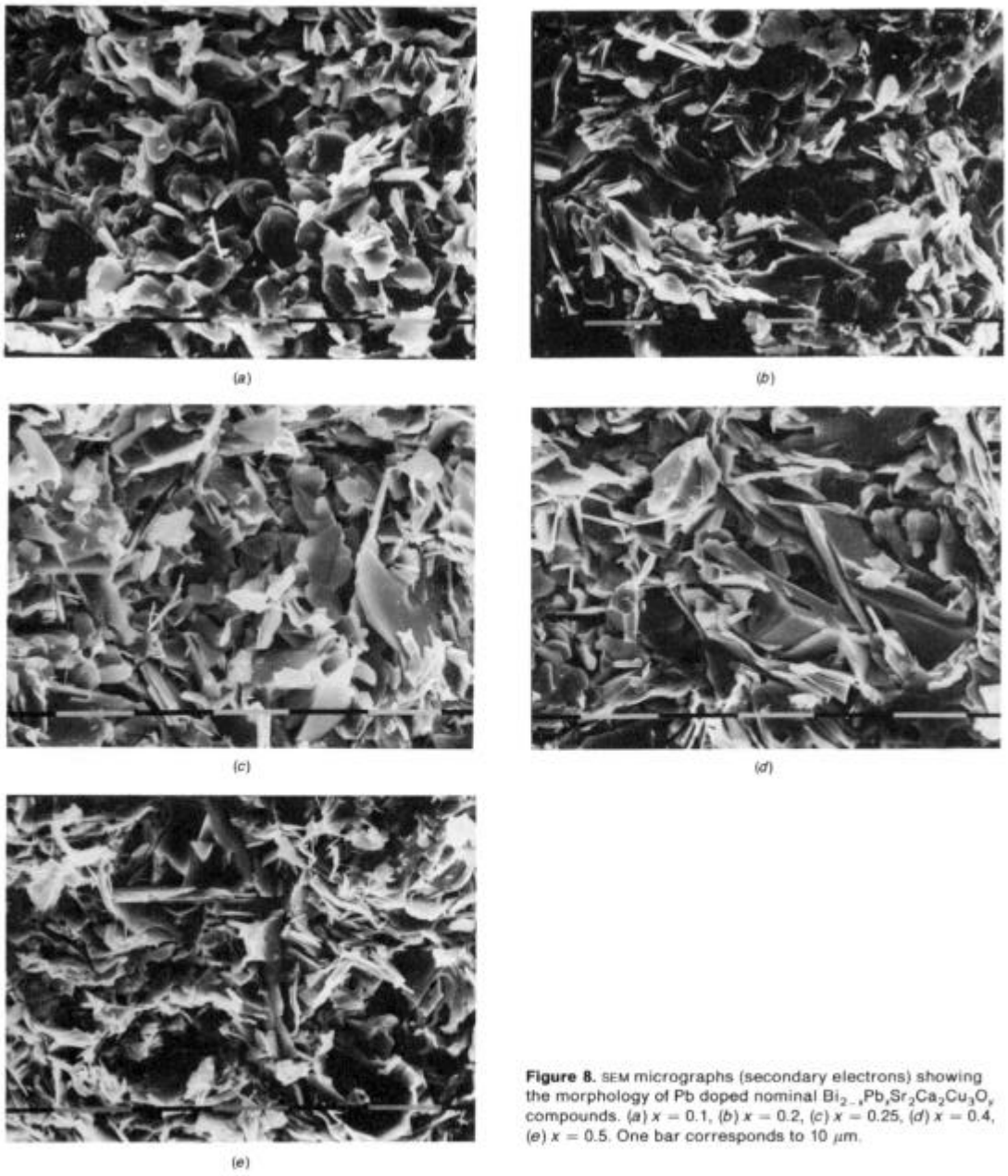

Figure 8. SEM micrographs (secondary electrons) showing the morphology of Pb doped nominal $Bi_{2-x}Pb_xSr_2Ca_2Cu_3O_y$ compounds. (*a*) $x = 0.1$, (*b*) $x = 0.2$, (*c*) $x = 0.25$, (*d*) $x = 0.4$, (*e*) $x = 0.5$. One bar corresponds to 10 μm.

pounds with $x = 0.1$, 0.2, 0.25, 0.4 and 0.5 from a fractured surface of the sintered material. The grains are plate-like. In figure 8 we can observe a gradual increase of the size of the plate-like grains from $x = 0.1$ to 0.4. There is also a certain degree of preferred orientation among the lamella crystals although it is far from perfect. Analysis of the stoichiometry gives results very close to the nominal stoichiometry although the Bi or Pb concentration is very difficult to estimate separately. The quantitative values for EDAX analysis have to be taken rather cautiously because of a lack of good standards.

4. Conclusions

We have studied the role of Pb concentration in the synthesis of the 2223 high-T_c superconductor in samples

with nominal stoichiometry $Bi_{2-x}Pb_xSr_2Ca_2Cu_3O_y$ for $x = 0.1, 0.2, 0.25, 0.3, 0.4, 0.5$ and investigated the conditions for growth of the high-T_c phase by controlling the sintering time and temperature.

The best sample was obtained by sintering in air for 350 h and at temperatures between 860–875 °C, for x values between 0.2 and 0.3 (see table 1 and figures 1–5). Sintering for longer than 100 h in step 6 does not change the form of the x-ray diffraction patterns.

The thermal process of the first three stages is needed for the calcination, homogenisation and transformation of the whole material into the 2212 phase, which in the following steps will be transformed into the 2223 phase.

It is worth noticing that sintering at 865 °C leads to partial melting of the sample, which attacks the Al_2O_3 crucible resulting in the deterioration of the initial chemical composition of the material. With the 'step sintering' process this difficulty is avoided and it is possible to obtain the best control over the thermal process because transformation of the material into the 2212 phase has occurred; hence the phases with a lower melting point of 875 °C are minimised and therefore the possibility of the material to melt while sintering at 860–875 °C at the final stage is reduced.

The growth rate of the 2223 phase in the samples with some Pb in the place of Bi is faster than the rate in samples with Bi only, and slower than the growth rate in samples with some (Pb, Sb) in the place of Bi [15].

We did not see any change in the crystallographic constants of the 2223 phase, within the limit of the resolution of our instrument. No straightforward relationship can be obtained between the value and shape of the electrical resistivity curve as a function of temperature and the amount of Pb which substitutes the Bi. Prolonged annealing time makes the system more metallic like.

Finally, the magnetic behaviour of the $Bi_{2-x}Pb_xSr_2Ca_2Cu_3O_y$ samples is related directly to the ratio 2223/2212, and this ratio closely depends on the percentage of Pb.

Acknowledgment

We would like to acknowledge Ames Laboratory for providing some of the oxides used in this work.

References

[1] Bednorz J G and Müller K A 1986 *Z. Phys.* B **64** 189
[2] Wu M K, Ashburn J R, Torng C J, Hor P H, Meng R L, Gao L, Huang Z J, Wang Y Q and Chu C W 1987 *Phys. Rev. Lett.* **58** 908
[3] Michel C, Hervieu M, Borel M M, Grandin A, Deslandes F, Provost J and Raveau B 1987 *Z. Phys.* B **68** 421
[4] Maeda H, Tanaka Y, Fukutomi M and Asano T 1988 *Japan. J. Appl. Phys. Lett.* **4** L209
[5] Torardi C C, Subramanian M A, Calabrese J C, Gopalakrishnan J, McCarron E M, Morrissey K J, Askew T R, Flippen R B, Chowdhry U and Sleight A W 1988 *Phys. Rev.* B **38** 225
[6] Tarascon J M, Le Page Y, Barboux P, Bagley B G, Greene L H, McKinnon W R, Hull G W, Giroud M and Hwang D M 1988 *Phys. Rev.* B **37** 9382
[7] Tarascon J M, McKinnon W R, Bardoux P, Hwang D M, Bagley B G, Greene L H, Hull G W, Le Page Y, Stoffel N and Giroud M 1988 *Phys. Rev.* B **38** 8885
[8] Torardi C C, Subramanian M A, Calabrese J C, Gopalakrishnan J, Morrissey K J, Askew T R, Flippen R B, Chowdhry U and Sleight A W 1988 *Science* **240** 631
[9] Cava R J *et al* 1988 *Physica* C **153–155** 560
[10] Yamada Y and Murase S 1988 *Japan. J. Appl. Phys.* **27** L996
[11] Green S M, Jiang C, Mei Yu, Luo H L and Politis C 1988 *Phys. Rev.* B **38** 5016
[12] Statt B W, Wang Z, Lee M J G, Yakhmi J V, de Camargo P C, Major J F and Rutter J W 1988 *Physica* C **156** 251
[13] Murayama N, Sudo E, Awano M, Kani K and Torii Y 1988 *Japan. J. Appl. Phys.* **27** L1629
[14] Balachandran U, Shi D, Dos Santos D I, Graham S W, Patel M A, Tani B, Vandervoort K, Claus H and Poeppel R B 1988 *Physica* C **156** 649
[15] Pissas M and Niarchos D 1989 *Physica* C **159** 643
[16] Maeda T, Sakuyama K, Yamauchi H and Tanaka S 1989 *Physica* C **159** 784